Journal of Solid State Chemistry 184 (2011) 2790–2793

Contents lists available at SciVerse ScienceDirect

Journal of Solid State Chemistry

journal homepage: www.elsevier.com/locate/jssc

Superstructure and stacking faults in hydrothermal-grown $KBe_2BO_3F_2$ crystals

Jinqiu Yu [a,b], Lijuan Liu [a,*], Shifeng Jin [c], Haitao Zhou [d], Xiaoling He [d], Changlong Zhang [d], Weining Zhou [d], Xiaoyang Wang [a], Xiaolong Chen [c], Chuangtian Chen [a]

[a] Beijing Center for Crystal Research and Development, Technical Institute of Physics and Chemistry, Chinese Academy of Sciences, P. O. Box 2711, Beijing 100190, China
[b] Graduate University of Chinese Academy of Sciences, Beijing 100039, China
[c] Beijing National Laboratory for Condensed Matter Physics, Institute of Physics, Chinese Academy of Sciences, Beijing 100190, China
[d] Guilin Research Institute of Geology for Mineral Resources, Guilin 541004, China

ARTICLE INFO

Article history:
Received 23 April 2011
Received in revised form
30 July 2011
Accepted 21 August 2011
Available online 26 August 2011

Keywords:
$KBe_2BO_3F_2$
Superstructure
Stacking faults

ABSTRACT

The structure of the hydrothermal-grown nonlinear optical crystal $KBe_2BO_3F_2$ was investigated. A new structure of the $R\bar{3}c$ space group with cell parameters of $a=4.422(1)$ Å and $c=37.524(3)$ Å was obtained by powder X-ray diffraction and Rietveld refinement. The new structure is a $1\times1\times2$ superstructure of the previously reported $R32$ structure with a different stacking sequence of $(Be_2BO_3F_2)_\infty$ layers along the c axis. The relationship between the refined structure and the experimental results is discussed. A stacking fault mechanism is proposed for the formation of the superstructure as well as the nonuniformity of the hydrothermal-grown KBBF crystals.

1. Introduction

$KBe_2BO_3F_2$ (KBBF) is currently one of the most excellent nonlinear optical (NLO) crystals in deep ultraviolet (DUV) harmonic generation. It can produce both tunable 4th harmonic generation of Ti:sapphire lasers and 6th harmonic generation of Nd-based lasers by a simple second harmonic generation (SHG) method. Detailed descriptions of its growth, space structure, optical properties and important applications were reviewed in Ref. [1]. The major disadvantage of KBBF is the crystal growth. Large sizes of high quality single crystals are very difficult to obtain, which seriously affects further applications.

There are two methods to grow KBBF crystals nowadays, by flux and by hydrothermal growth. The former method can produce crystals of good optical quality. All the important crystallographic data and NLO properties of KBBF were determined from the flux grown crystals. However, due to the strong layered growth tendency, the thickness of the as-grown crystals along the c axis is limited, which hampers many applications. The hydrothermal growth of KBBF was developed in recent years and can yield much thicker crystals [2–4], which were reported to have the same $R32$ structure as the flux grown ones [2,3], but their SHG conversion efficiency was found much lower [1]. The reason for this is still unclear, and no related research has been reported except for ours [5].

Our earlier study revealed that the powder X-ray diffraction (PXRD) patterns of the hydrothermal-grown KBBF crystals usually contain three tiny extra peaks, which cannot be indexed by the $R32$ structure. The intensities of these extra peaks differ for different crystal samples. The stronger the extra peaks, the lower the powder SHG intensity of the crystal [5]. This was attributed to some structural defects, but no detailed explanation could be given at that time. In this paper, recent progress in this respect is introduced. The extra peaks were attributed to superstructure reflections and a new structure of $R\bar{3}c$ space group was obtained by PXRD and Rietveld refinement. The new structure together with a stacking fault mechanism can finely explain all the experimental results observed for hydrothermal-grown KBBF crystals, and may give us some new insight about the structure of similar boron materials.

2. Experiments

KBBF crystals were grown by both flux and hydrothermal methods [4,6]. The hydrothermal crystals were grown from $KF+H_3BO_3$ or KOH solutions with seeds. The growth temperature was about 410–430 °C and the fill rate was about 75% with a pressure reaching 120 Mpa. The growth period was about 30–60 days. An as-grown KBBF crystal is shown in Fig. 1.

* Corresponding author. Fax: +86 1082543709.
E-mail address: llj@mail.ipc.ac.cn (L. Liu).

0022-4596/$ - see front matter © 2011 Elsevier Inc. All rights reserved.
doi:10.1016/j.jssc.2011.08.025

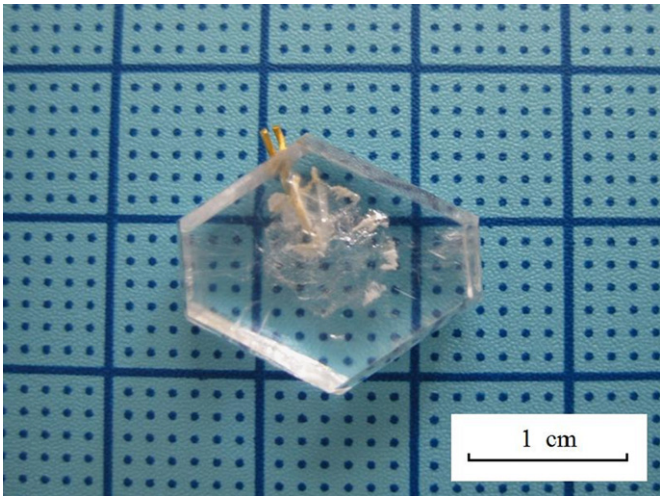

Fig. 1. An hydrothermal-grown KBBF crystal.

Different hydrothermal-grown KBBF crystal samples were ground into powder for X-ray diffraction and SHG intensity tests according to Kurtz and Perry's method [7]. The same experiments were performed on flux grown KBBF crystals for comparison.

A transparent hydrothermal-grown KBBF crystal with obvious extra peaks revealed by PXRD was chosen for structure determination and refinement. The PXRD data was collected on a PANalytical X-ray diffractometer (X'Pert PRO MRD) using Cu$K\alpha$1 radiation (λ=1.54056 Å) and a graphite monochromator in the reflection mode (2θ=10–110°, step width=0.033° and scan speed=21 s/step) at room temperature. A capillary sample holder was used due to the strong orientation preference of the powders. The refinement was carried out by the Rietveld method [8] with the Fullprof program [9].

The PXRD simulations of stacking faults were performed with the DIFFaX software [10,11].

3. Results and discussions

3.1. Structure refinement and descriptions

As mentioned above, the PXRD patterns of the hydrothermal-grown KBBF crystals usually contain some tiny extra peaks, which cannot be indexed by the $R32$ structure, with the three most obvious ones located at ~41.4°, 46.5° and 55.4°. Using powder cell analysis, it was found that doubling the unit cell along the c-axis could index the three main additional peaks well, which indicates that they could be referred to superstructure reflections. This made us consider the possibility of other subgroups of the trigonal system based on a $1\times1\times2$ superstructure of the $R32$ structure. A good fitting result with R_p/R_{wp}=3.65%/4.79% was finally obtained when the $R\bar{3}c$ symmetry was chosen. The cell parameters were refined to be a=4.422(1) Å and c=37.524(3) Å, while the parameters of the $R32$ space group are a=4.427(4) Å and c=18.744(9) Å. The final refinement pattern is given in Fig. 2. The three extra peaks are indexed to be (1 1 3), (1 1 9), and (1 1 15). The crystallographic data, structure refinement and atom parameters of the $R\bar{3}c$ structure are listed in Tables 1 and 2. More detailed structure information is provided in Supplemental Data.

The $R\bar{3}c$ structure is centrosymmetric and therefore has no SHG effect. Compared to the $R32$ structure, the $R\bar{3}c$ structure has the same anionic groups of $(BO_3)^{3-}$ triangles and $(BeO_3F)^{5-}$ tetrahedra as fundamental building units. They form into $(Be_2BO_3F_2)_\infty$ layers along the a–b plane with all the $(BO_3)^{3-}$ triangles parallel and

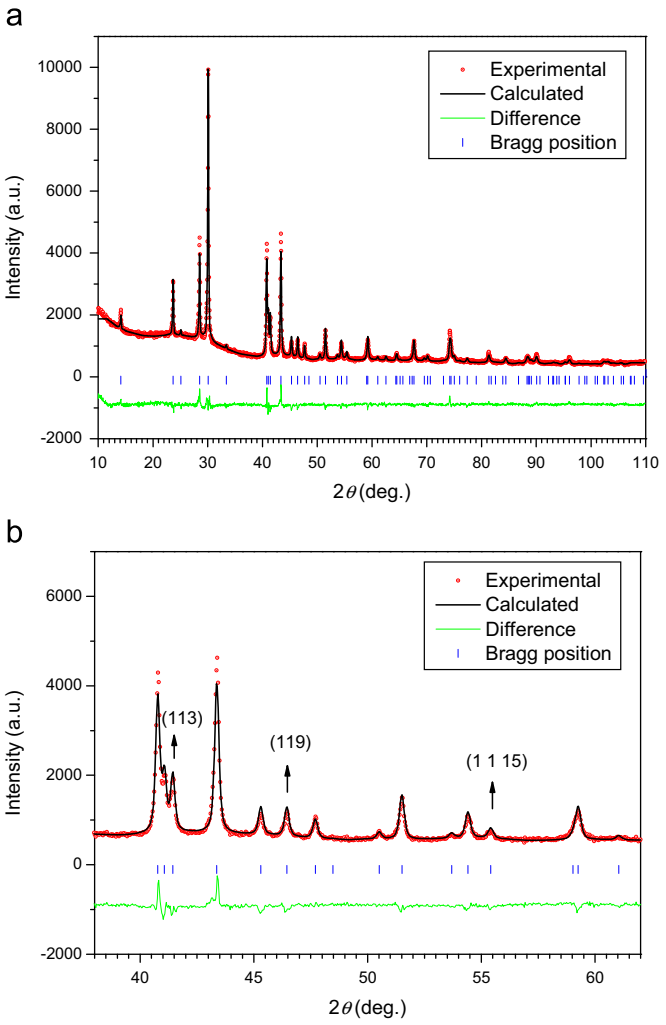

Fig. 2. Final Rietveld refinement plot of the $R\bar{3}c$ structure. (a) Whole range of 2θ (10–110°) while (b) is for part of it. The three marked peaks in (b) are the extra ones, which cannot be indexed by the $R32$ structure. They are indexed to be (1 1 3), (1 1 9) and (1 1 15) by the $R\bar{3}c$ structure.

F atoms above or below the plane. The connection of these anionic groups and the layered construction are nearly the same. However, the arrangement of the planar $(BO_3)^{3-}$ groups between adjacent $(Be_2BO_3F_2)_\infty$ layers are slightly different. As illustrated in Fig. 3, there are six $(Be_2BO_3F_2)_\infty$ layers in each $R\bar{3}c$ unit cell and each layer has one $(BO_3)^{3-}$ group. Among them, three layers of $(BO_3)^{3-}$ groups have the same direction A and the other three layers of them are in the opposite direction B (rotated 60° along the c axis). The stacking sequence of the layers is ABABAB. By contrast, all the $(BO_3)^{3-}$ groups have the same direction in the $R32$ structure with a stacking sequence of AAA. According to the anionic group theory [12], the SHG coefficient of KBBF mainly comes from the $(BO_3)^{3-}$ groups, and the twisted arrangement of adjacent $(BO_3)^{3-}$ groups in the $R\bar{3}c$ structure will lead to an offset of the overall SHG coefficient.

3.2. Crystal nonuniformity and stacking faults

The PXRD and powder SHG tests revealed that the hydrothermal-grown KBBF crystals are of severe nonuniformity. Different crystal samples differ in both PXRD patterns and powder SHG intensities, even when they are from the same bulk crystal. The refined structure was obtained from the crystal with the most obvious extra peaks, but in most of the crystal samples these

Table 1
Crystallographic data, experimental details of powder X-ray diffraction and Rietveld refinement data for hydrothermal-grown KBBF.

Chemical formula	$KBe_2BO_3F_2$
Formula weight	153.93
Crystal system	Trigonal
Space group	$R\bar{3}c$ (no.167)
a (Å)	4.422(1)
c (Å)	37.524(3)
Volume (Å^3)	635.4(3)
Z	6
d_c (g/cm^3)	2.413
Diffractometer	PANalytical X'Pert Pro MRD
Radiation type	Cu$K\alpha$1
Wavelength (Å)	1.54056
Profile range (°2θ)	10–110
Step size (°2θ)	0.033
Number of observation (N)	3030
Number of contributing reflections	396
Number of structure parameters (P_1)	7
Number of profile parameters (P_2)	8
R_{Bragg} (%)	10.3
R_p (%)	3.65
R_{wp} (%)	4.79
R_{exp} (%)	3.47

Note: $R_p=\Sigma|y_{io}-y_{ic}|/\Sigma|y_{io}|$, $R_{wp}=[\Sigma w_i(y_{io}-y_{ic})^2/\Sigma w_i y_{io}^2]^{1/2}$, $R_{exp}=[(N-P_1-P_2)/\Sigma w_i y_{io}^2]^{1/2}$, $S=\Sigma[w_i(y_{io}-y_{ic})^2/(N-P_1-P_2)]^{1/2}$.

Table 2
Atom parameters for hydrothermal-grown KBBF.

Atom	x	y	z	U_{eq} (Å^2)
K1	0.00000	0.00000	0.00000	0.0246 (8)
Be1	0.00000	0.00000	0.0988 (1)	0.054 (4)
B1	−0.33333	−0.66667	0.08333	0.029 (4)
O1	−0.33333	−0.9762 (3)	0.08333	0.0628 (16)
F1	0.00000	0.00000	0.36086 (7)	0.0537 (17)

peaks are much weaker, sometimes even indiscernible. For the crystals with obvious extra peaks, the powder SHG intensity was measured to be only 3% that of the flux grown ones, while for those with weaker and indiscernible extra peaks, they were 29% and 43%, respectively [5]. For the crystals with obvious extra peaks, the $R\bar{3}c$ structure agrees well with the experimental results both in PXRD patterns and powder SHG intensities and therefore can make an acceptable explanation, but for those with weaker and indiscernible extra peaks, more explanations are still needed.

The hydrothermal-grown KBBF crystals are not simple mixtures of the $R32$ and $R\bar{3}c$ structures as macroscopic isomers, since it is very difficult to peak up a perfect millimeter-scale single crystal of either structure, and we failed to obtain the $R\bar{3}c$ structure by single crystal diffraction. They are more likely to be microscopic intergrowth of the two structures. Since some hydrothermal crystals were grown with seeds from flux grown KBBF, we particularly examined the remaining seeds of them by PXRD, and found them keep the same as the $R32$ structure. This indicates that the $R\bar{3}c$ structure should be formed during the growth process.

Based on the above analyses, we presume that the crystal nonuniformity was caused by stacking faults during the hydrothermal growth process. Taking the flux grown $R32$ structure with $(Be_2BO_3F_2)_\infty$ layers of aligned $(BO_3)^{3-}$ groups as a perfect model, a $(Be_2BO_3F_2)_\infty$ layer with twisted $(BO_3)^{3-}$ groups can be seen as a stacking fault. Considering the layered structure and the weak combination between the adjacent $(Be_2BO_3F_2)_\infty$ layers, such stacking faults could be introduced easily along the c axis. With the DIFFaX software, we simulated the PXRD patterns with different incidences of the stacking faults. We built the stacking

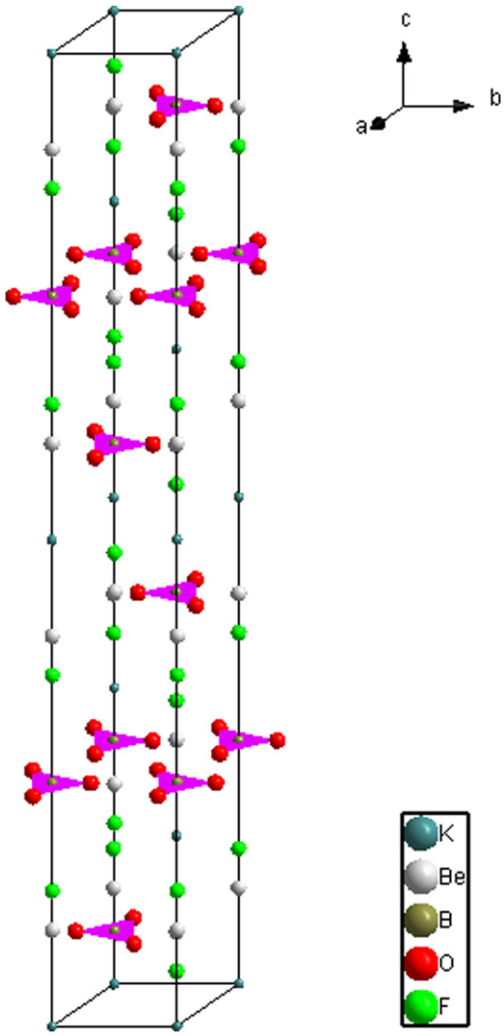

Fig. 3. Unit cell of the $R\bar{3}c$ structure. Triangles are $(BO_3)^{3-}$ groups.

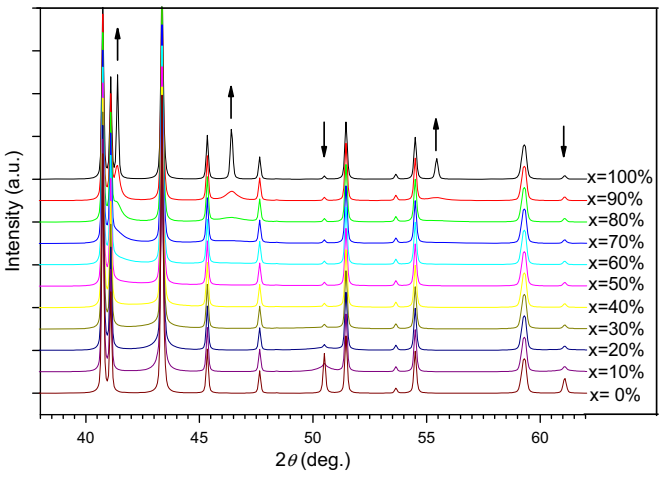

Fig. 4. Simulated XRD patterns with different stacking fault incidence.

model as …AX…, where A represents one $(Be_2BO_3F_2)_\infty$ layer, and X represents a possible reversed stacking with an incidence of x. For examples, x=0% results in the stacking sequence of …AAAAAA… ($R32$), while x=100% results in …ABABAB… ($R\bar{3}c$). The simulated result is shown in Fig. 4. As the stacking fault incidence rises, the intensity of the three extra peaks (marked by up arrows) goes up

with two other peaks (marked by down arrows) going down, which agrees quite well with the experiments. This simulation also reveals that the extra peaks can only be observed when the stacking fault incidence is more than 80%. This can finely explain why some hydrothermal-grown KBBF crystals have much lower powder SHG intensity even though their PXRD patterns look quite the same as the flux grown ones. Thus, the nonuniformity of the hydrothermal-grown KBBF crystals can be simply attributed to the varying density of the stacking faults. The higher the concentration of the stacking faults, the more obvious the extra peaks in PXRD, and the lower SHG coefficient of the crystal.

We tried to confirm our assumption by electron diffraction and high resolution lattice imaging with transmission electron microscopy, but unfortunately failed due to two reasons. One is that the hydrothermal-grown KBBF crystals cleave so easily along the *c* axis that samples of desired orientations can hardly be prepared. The other is that the crystals cannot sustain the high energy electron beam and easily get molten and decomposed, which makes the observation rather difficult. More efforts are still needed for further experimental evidence.

It is worth noting that this nonuniformity only exists in hydrothermal-grown KBBF crystals and has not been found in flux grown crystals so far. This indicates that the stacking faults are more likely to happen under hydrothermal conditions. It is still unknown whether they could be eliminated by improving the growth technique.

The structural problem of hydrothermal-grown KBBF is quite similar to that of the $Na_2Al_2B_2O_7$ (NABO) [13–15] and $Sr_2Be_2B_2O_7$ (SBBO) [16,17] family crystals. They share a common structural characteristic of a layered $[M_2B_2O_7]_\infty$ (M=Al, Be) network formed by parallel BO_3 triangles combined with MO_4 tetrahedra. For KBBF, the BeO_4 tetrahedra are replaced by BeO_3F, while the layered structure is nearly the same. Though twins and domain structures caused by stacking faults were proposed to explain the structural complexity of NABO and SBBO crystals and did agree well with some theoretical calculations [14,15,17], they have not been confirmed by convincing experimental evidence yet. Structures of these crystals are still not well understood. This investigation on hydrothermal-grown KBBF may also be helpful for structure study of NABO and SBBO family crystals.

4. Conclusions

The structure of the hydrothermal-grown KBBF crystals was investigated by PXRD and Rietveld refinement. A new structure of the $R\bar{3}c$ space group was obtained, which is a $1\times1\times2$ superstructure of the previously reported $R32$ structure. The formation of the superstructure is considered to be caused by stacking faults, which may also account for the nonuniformity of the hydrothermal-grown KBBF crystals. This work may be helpful for future structural investigations of similar boron materials.

Acknowledgments

This work was financially supported by the National Natural Science Foundation of China under Grant no. 50590402, the National Basic Research Project of China (2010CB630701) and the Guangxi Natural Science Foundation (0832020).

Appendix A. Supplementary materials

Supplementary data associated with this article can be found in the online version at doi:10.1016/j.jssc.2011.08.025.

References

[1] C.T. Chen, G.L. Wang, X.Y. Wang, Z.Y. Xu, Appl. Phys. B 97 (2009) 9–25.
[2] Ning Ye, Dingyuan Tang, J. Cryst. Growth 293 (2006) 233–235.
[3] Colin D. McMillen, Joseph W. Kolis, J. Cryst. Growth 310 (2008) 2033–2038.
[4] H.T. Zhou, X.L. He, et al., J. Cryst. Growth 318 (2011) 613–617.
[5] J.Q. Yu, L.J. Liu, X.Y. Wang, H.T. Zhou, X.L. He, C.L. Zhang, W.N. Zhou, C.T. Chen, J. Cryst. Growth 318 (2011) 621–624.
[6] X.Y. Wang, X. Yan, S.Y. Luo, C.T. Chen, J. Cryst. Growth 318 (2011) 610–612.
[7] S.K. Kurtz, T.T. Perry, J. Appl. Phys. 39 (1968) 3798–3813.
[8] H.M. Rietveld, Acta Crystallogr. 22 (1967) 151–152.
[9] J. Rodriquez-Carvajal, M.T. Fernadez-Diaz, J.L. Martinez, J. Phys.: Condens. Matter 3 (1991) 3215–3234.
[10] M.M.J. Treacy, J.M. Newsam, M.W. Deem, Proc. R. Soc. Lond. A433 (1991) 499–520.
[11] T.N. Ramesh, P. Vishnu Kamath, C. Shivakumara, Acta Cryst. B62 (2006) 530–536.
[12] C.T. Chen, N. Ye, J. Lin, J. Jiang, W.R. Zeng, B.C. Wu, Adv. Mater. 11 (1999) 1071–1078.
[13] M. He, X.L. Chen, T. Zhou, B.Q. Hu, Y.P. Xu, T. Xu, J. Alloys Compds. 327 (2001) 210–214.
[14] M. He, L. Kienle, A. Simon, X.L. Chen, V. Duppel, J. Solid State Chem. 177 (2004) 3212–3218.
[15] X.Y. Meng, J.H. Gao, Z.Z. Wang, R.K. Li, C.T. Chen, J. Phys. Chem. Solids 66 (2005) 1655–1659.
[16] C.T. Chen, Y.B. Wang, B.C. Wu, K.C. Wu, W.L. Zeng, L.H. Yu, Nature 373 (1995) 322–324.
[17] C.T. Chen, L. Bai, Z.Z. Wang, R.K. Li, J. Cryst. Growth 292 (2006) 169–178.